Title: Ecosystem-scale spatial heterogeneity of stable isotopes of soil nitrogen in African savannas

Running title: Soil ^{15}N spatial pattern

Article type: Regular Research Article

Authors: Lixin Wang[a, b*], Gregory S. Okin[c], Paolo D'Odorico[d], Kelly K. Caylor[e] and Stephen A. Macko[d]

a. Department of Earth Sciences, Indiana University-Purdue University, Indianapolis (IUPUI), Indianapolis, Indiana 46202, USA

b. Water Research Center, School of Civil and Environmental Engineering, University of New South Wales, Sydney, NSW, 2052, Australia

c. Department of Geography, 1255 Bunche Hall, University of California, Los Angeles, CA 90095, USA

d. Department of Environmental Sciences, University of Virginia, Charlottesville, VA, 22904, USA

e. Department of Civil and Environmental Engineering, Princeton University, Princeton, NJ, 08544, USA

Date of the manuscript draft: June 25 2012

Manuscript word count (including text and references): 6542

*Corresponding author
Lixin Wang
School of Civil and Environmental Engineering
University of New South Wales, Sydney, NSW, 2052, Australia
E-mail: w.lixin@gmail.com
Telephone: 61-(02)-9385 5227

This is the author's manuscript of the article published in final edited form as:

Wang, L., Okin, G. S., D'Odorico, P., Caylor, K. K., & Macko, S. A. (2013). Ecosystem-scale spatial heterogeneity of stable isotopes of soil nitrogen in African savannas. Landscape ecology, 28(4), 685-698.
http://dx.doi.org/10.1007/s10980-012-9776-6

Abstract

Soil ^{15}N is a natural tracer of nitrogen (N) cycling. Its spatial distribution is a good indicator of processes that are critical to N cycling and of their controlling factors integrated both in time and space. The spatial distribution of soil $\delta^{15}N$ and its underlying drivers at sub-kilometer scales are rarely investigated. This study utilizes two sites (dry vs. wet) from a megatransect in southern Africa encompassing locations with similar soil substrate but different rainfall and vegetation, to explore the effects of soil moisture and vegetation distribution on ecosystem-scale patterns of soil $\delta^{15}N$. A 300-m long transect was set up at each site and surface soil samples were randomly collected for analyses of $\delta^{15}N$, %N and nitrate content. At each soil sampling location the presence of grasses, woody plants, *Acacia* species (potential nitrogen fixer) as well as soil moisture levels were recorded. A spatial pattern of soil $\delta^{15}N$ existed at the dry site, but not at the wet site. Woody cover distribution determined the soil $\delta^{15}N$ spatial pattern at ecosystem-scale; however, the two *Acacia* species did not contribute to the spatial pattern of soil $\delta^{15}N$. Grass cover was negatively correlated with soil $\delta^{15}N$ at both sites owing to the lower foliar $\delta^{15}N$ values of grasses. Soil moisture did not play a role in the spatial pattern of soil $\delta^{15}N$ at either site. These results suggest that vegetation distribution, directly, and water availability, indirectly, affect the spatial patterns of soil $\delta^{15}N$ through their effects on woody plant and grass distributions.

Keywords: C_3 plants, C_4 plants, Geostatistics, Isotope, Kalahari, Savannas, Soil $\delta^{15}N$, Soil nitrogen, Stable isotopes

1. Introduction

Soil ^{15}N is a natural integrator of soil nitrogen (N) cycling processes (Högberg 1997; Robinson 2001). Fundamentally, soil $\delta^{15}N$ values are imposed by the isotopic compositions of N inputs (e.g., through N fixation and leaf litter decomposition), fractionations associated with N transformations (e.g., mineralization, nitrification and diagenesis) and N losses (e.g., denitrification and volatilization).

Factors influencing soil $\delta^{15}N$ values can be classified as direct factors when they affect the soil $\delta^{15}N$ through their impact on N inputs, transformations or losses. For example, vegetation affects the soil $\delta^{15}N$ value through litter decomposition and N fixation. The fixed N in soil could either come from vegetation (e.g., N fixing trees or forbs) or from soil crusts especially in drylands (Evans and Ehleringer 1993; Aranibar et al. 2003). Soil N transformation processes such as ammonification, ammonia volatilization, coupled nitrification-denitrification will also have significant impact on soil $\delta^{15}N$ values. It is worth noticing that some processes could be less important in certain conditions. For instance, if the pH values are low (e.g., soils are acidic), ammonia volatilization will be minimum. Besides the direct factors, the soil $\delta^{15}N$ values depend also on other indirect factors such as soil topography (Garten and Van Miegroet 1994; Bai et al. 2009) and rainfall (Aranibar et al. 2004; Swap et al. 2004; Wang et al. 2010a). These factors are related to N transformations and losses through their impact on the soil water balance and can therefore indirectly affect soil $\delta^{15}N$ values. For instance, soil moisture dynamics strongly control soil N transformations in drylands (Austin et al. 2004; Wang et al. 2009a). Because ^{15}N is one component of total N, soil $\delta^{15}N$ dynamics are also influenced by soil moisture variations.

The spatial distribution of soil $\delta^{15}N$ values therefore results from the integration of both the direct and indirect factors. At watershed scales, soil $\delta^{15}N$ has been found to be slightly higher on south facing slopes, compared with ridges, valley bottoms and north facing slopes in the northern hemisphere (Garten 1993). The soil $\delta^{15}N$ values of extractable soil NH_4^+ and NO_3^-, however, were much higher at the valley bottoms than other locations, because of the higher rates in mineralization and nitrification at valley bottoms (Garten 1993), which fractionated ^{15}N and made the residuals enriched. The higher mineralization and nitrification rates were likely linked to higher water availability at the valley bottoms. At regional scale, soil $\delta^{15}N$ values have been used to correlate with N deposition because soil $\delta^{15}N$ increases when N deposition induced nitrification and nitrate loss increase (Pardo et al. 2007). At the global scale, the soil $\delta^{15}N$ spatial distribution has been empirically related to climatic parameters such as mean annual temperature and mean annual precipitation (Amundson et al. 2003). Recent studies have explored the possibility of predicting foliar $\delta^{15}N$ (closely related to soil $\delta^{15}N$) using remote sensed spectral data (Wang et al. 2007a; Elmore and Craine 2011), pointing out the possibility of direct estimate of large-scale $\delta^{15}N$ variations. Spatial patterns of soil $\delta^{15}N$ have rarely been investigated at the sub-kilometer to kilometer spatial scale (e.g., ecosystem-scale), especially with spatial-explicit samplings (vs. discreet sampling) (e.g., Cheng et al. 2009; Bai et al. 2009). The interpretation of such ecosystem-scale distribution of $\delta^{15}N$ is partly complicated by the complex interactions and synergic effects between direct and indirect factors, whereby both vegetation distribution and soil moisture could affect $\delta^{15}N$ patterns and these two factors could also interact with each other. At the same time, processes such as mineralization, nitrification and denitrification

affect the δ^{15}N spatial pattern at small scales. Because these processes are all directly or indirectly related to the presence of vegetation, at larger scales their overall effects may be investigated through a few aggregated indicators such as woody cover and grass cover. This approach simplifies the ecosystem-scale soil δ^{15}N estimation without necessarily evaluating in detail all the processes involved in N cycling. The investigation of soil δ^{15}N spatial patterns at the ecosystem-scale and the exploration of the underlying mechanisms are therefore critically needed to bridge the gap existing between δ^{15}N measurements at different scales.

In the present study, we aimed to explore 1) whether there are spatial patterns in soil δ^{15}N at a large spatial scale (e.g., sub-kilometer scale); and 2) how soil moisture and woody vegetation - particularly potential N-fixing species - interactively control the spatial distribution of soil δ^{15}N at this scale (in case soil δ^{15}N spatial patterns are observed). To this end, we used the Kalahari Transect (KT) as a model system. The KT is one of a set of IGBP (International Geosphere-Biosphere Programme) "megatransects" (Koch et al. 1995) identified for global change studies. There are several unique aspects of this transect making it ideal for the ecosystem-scale characterization of the spatial patterns of soil δ^{15}N: 1) the soil substrate consists of Kalahari sands, which are consistent and homogeneous along the entire transect (Wang et al. 2007b); 2) the topography across the transect is flat with gentle slopes (<1%), minimizing the interactive effects of rainfall and topography on soil moisture. In the south (the dry end of the transect), it is a fine-leaf savanna with several potential N-fixers such as *Acacia mellifera* Benth. and *A. leuderitzii* Engl. Vegetation in the north (the wet end) is dominated by broad-leaf woody species such as *Burkea africana*, *Ochna pulchra*, *Bauhimia macrantha*, which are not

potential N-fixers. According to an earlier report, using foliar δ^{15}N, C/N ratio and taxonomic classification as indication, there are potential N-fixing forbs and some potential N-fixing trees, such as *Baphia*, *Indigophera*, and *Tephrosia* at the wet end (Aranibar et al. 2004), but they are less common in the current study site. The mesic site considered in this study also does not exhibit N-fixing genera such as *Dalbergia*, *Dichrostachys, Entada* and *Xeroderris* that were found in Tanzania woodlands under similar rainfall regimes (Hogberg 1986). Soil crusts are also reported to fix N, but soil crust cover is low at the mesic site, probably due to anthropogenic disturbance based on field observations. The KT thus provides a species and rainfall contrasts to investigate ecosystem-scale soil δ^{15}N spatial patterns along a precipitation gradient while minimizing confounding effects of soil heterogeneity. Three hypotheses were tested: 1) soil δ^{15}N is spatially structured at both ends of the KT (dry vs. wet); 2) the spatial pattern of soil δ^{15}N is influenced by woody plant distribution at both ends of the KT. The first two hypotheses are based on the results of previous studies showing a relationship between the spatial distribution of woody plants and total soil N (Okin et al. 2008) and based on the positive relationships between total N and δ^{15}N in many non-N fixing dominant ecosystems (e.g., a global synthesis in Wang et al. 2009b); and 3) soil moisture affects the spatial distribution of soil δ^{15}N. This is based on the modeling and field observations showing the effect of soil moisture on soil N dynamics (e.g., Wang et al. 2009a) as well as the positive relationships between total N and δ^{15}N in non-N fixing dominant ecosystems (Wang et al. 2009b). Supposedly higher soil moisture will lead to higher

mineralization and nitrification rates (Austin et al. 2004), since mineralization/nitration fractionate ^{15}N, the residuals will be enriched.

2. Materials and Methods

2.1 Field sites and field samplings

The mean annual precipitation (MAP) along the KT ranges from less than 200 mm in the south to over 1000 mm in the north. The physical parameters such as soil texture (>96% of sand) and bulk density (around 1.4-1.5 g cm^{-3} along the whole transect) do not have significant variations along the KT (Wang et al. 2007b; Thomas et al. 2008). Two sites in the Botswana part of the Kalahari (Figure 1) with different mean MAP (near the extreme MAPs along the KT) were chosen to compare the spatial patterns of soil $\delta^{15}N$ and explore the underlying mechanisms of such patterns. The southern site, Tshane, is at the dry end of the transect (~365 mm MAP) and the northern site, Mongu, is wetter (~900 mm MAP). The Tshane site is classified as open savanna dominated by *Acacia* species such as *A. luederizii* and *A. mellifera* whereas the dominant grass species are *Eragrostis lehmanniana* and *Schmidtia pappophoroides*. The Mongu site is located in a woodland savanna dominated by tree species such as *Brachystegia spiciformis* Benth and the *Eragrostis spp.* grass species. The *A. luederizii* and *A. mellifera* species found in Tshane are potential N fixers, though their foliar $\delta^{15}N$ reaches 8‰, suggesting that they may not rely heavily on atmospheric N as their major N source at the this site (Wang et al. 2010a). The sampling was conducted in February-March, 2005. The rainfall was 436 mm in Tshane, higher than the MAP of the site, and 564 mm in Mongu in 2005, lower than the MAP of the site. The 2005 rainfall data was from Tropical Rainfall Measuring Mission (TRMM), and was reported earlier (Wang et al. 2010b). Five individual trees and grasses

were randomly selected at each site, foliar and root samples (0-30 cm and 30-50 cm for trees, 0-30 cm for grasses) were collected. For grasses, the whole individual was collected for foliar samples; for trees, 5-10 leaves were collected from each tree at 1.5 m height. The tree species in Tshane was *A. mellifera* and grass species were *Schmidtia pappophoroides*, *Eragrostis lehmanniana*, *Stipagrostis suniplumis* and *Aristida congesta*. The species at Mongu were not identified.

A 300-m line transect was set up at each site and surface soil samples (0-5 cm depth) were randomly collected along the transect (with a ~1 m interval on average, 220 samples from each site). The sampling locations were selected along the transect using a random number generator with uniform distribution. The irregular spacing of samples along the transect allowed us to calculate semivariograms relying on a relatively large number of points that are closely spaced. While performing the random soil sampling along each transect, the presence/absence (in binary form) of trees and shrubs (C_3 vegetation) or of grasses and forbs (C_4 vegetation) as well as presence/absence of bare ground were recorded for each sampling point. Soil crust covers were low at both sites, presumably due to disturbance of local villagers, and were not recorded. Surface soil moisture (0-5 cm) was also measured at each sampling point using Time Domain Reflectometry (TDR, Campbell Scientific Inc., Logan, USA). The resolution is about 1%. Because of the onetime sampling, the soil moisture results are snapshot based and may not reflect the long-term values.

2.2 Laboratory analysis

All soil samples were oven dried at 60^{o}C in the laboratory, sieved to remove plant debris and homogenized using mortar and pestle. The soil C and N content was

measured using an Elemental Analyzer (EA, Carlo Erba, NA1500, Italy). The nitrate concentrations (including both NO_3^- and NO_2^- here) were analyzed using Dionex ICS-2000 ion chromatograph (Dionex, Sunnyvale, CA) with an Ion Pac AS 18 anion exchange column. The soil C and N as well as nitrate concentrations were reported in an earlier study (Okin et al. 2008). The stable N isotope analyses of plant foliar, root samples and soil were performed using an Optima Isotope Ratio Mass Spectrometer (IRMS) connected to the EA (GV/Micromass, Manchester, UK). Stable isotope compositions are reported in the conventional form:

$$\delta^{15}N\ (‰) = [(^{15}N/^{14}N)_{sample} / (^{15}N/^{14}N)_{standard} - 1\ ] \times 1000, \quad (1)$$

where $(^{15}N/^{14}N)_{sample}$ and $(^{15}N/^{14}N)_{standard}$ are the isotopic ratios of the sample and standard, respectively. The standard is atmospheric N_2. Reproducibility of these measurements is typically better than 0.2‰.

2.3 Statistical analysis

All data sets were tested for normality (SAS 9.1, SAS Inc., Cary, NC, USA) before performing conventional statistical and geostatistical analyses. Conventional statistics (i.e., mean and coefficient of variation (CV)) were calculated to investigate the overall variability for each analyzed variable. Geostatistical analyses were performed with the GS^+ software (Version 7.0, Gamma design software, Plainwell, MI, USA) to determine for each site the spatial variation of soil $\delta^{15}N$, %N, $NO_3^-+NO_2^-$, water content, and vegetation. Before the semivariogram computation, the data were tested for 1st or 2nd order trends (Davis 2002) and no trends were found.

A semivariogram (SV hereafter) is a plot of a series of semivariance values (γ) against the corresponding lag distances (h). The semivariance γ at each h is defined as:

$$\gamma(h)= \frac{1}{2N(h)}\sum_{i=1}^{N(h)}[z(i)-z(i+h)]^2, \quad (2)$$

where $N(h)$ is the number of sample pairs separated by the lag distance h. $z(i)$ is a value measured at location i and $z(i+h)$ is a value measured at location $i+h$. A number of models are commonly used to fit the calculated values of the SV, $\gamma(h)$. The model selection is based on two criteria: high R-square and the shape of the fitted model. Because in similar studies the spherical model was shown to provide an adequate representation of the spatial variability of soil data (Schlesinger et al. 1996; Su et al. 2006; Wang et al. 2007c), in this study the semivariograms of all the variables at the wet site (Mongu) were fitted by a spherical model. However, for the Tshane site the exponential model provides a better fit of the soil $\delta^{15}N$ data both in terms of shape and R-square value. Therefore, the exponential model was used for all the variables at the dry site (Tshane) to facilitate the comparison within this site. A 75 m lag distance and 1 m uniform interval were used for semivarigram calculations.

The spherical model is defined as:

$$\gamma(h) = C_o + C\,[1.5\,(h/A_o) - 0.5\,(h/A_o)^3] \text{ for } h \le A_o$$

$$\gamma(h) = C_o + C \text{ for } h > A_o, \quad (3)$$

The exponential model is defined as:

$$\gamma(h) = C_o + C\,[1 - \exp\,(-h/A_o)], \quad (4)$$

where C_o is nugget, A_o is range and h is lag distance interval.

Three SV parameters were derived and used in the analysis: nugget (C_o), range (A_o), the ratio of structure variance (C) and sill variance ($C + C_o$) ($C/(C+C_o)$, thereafter). Nugget reflects either the variability at scales finer than data resolution or variability due

to measurement or locational error. Range indicates the distance of spatial autocorrelation between data pairs. Samples separated by distances smaller than the range are correlated whereas samples separated by greater distance are independent. The value $C/(C+C_o)$ is the proportion of the total variance that is spatially structured. A high $C/(C+C_o)$ indicates that variability in the dataset is strongly structured (Brooker 1991; Wang et al. 2007c; Li et al. 2010). The uncertainties (95% confidence limits) of the derived parameters were determined using the variance-covariance method of Pardo-Inuzquiza (2001). The 95% confidence limits of these parameters were calculated using a code written in Interactive Data Language (IDL, Exelis Visual Information Solutions, Boulder, CO, USA) that was applied to earlier studies (Li et al. 2008; Okin et al. 2008; Wang et al. 2009c) and is available on request.

The spatial correlations of all the parameters were calculated with "modified *t*-test for correlation" using PASSAGE software package (http://www.passagesoftware.net/) developed by Rosenberg and Anderson (2011). This test corrects the degrees of freedom based on the amount of auto-correlation in the data (e.g., Wang et al. 2007c).

3. Results and Discussion

Figure 2 depicts the ecosystem-scale variations of $\delta^{15}N$ (A), soil %N (B), soil C/N (C), soil $NO_3^-+NO_2^-$ (D) and soil moisture (E) at Tshane and Mongu. Soil $\delta^{15}N$ is higher at the Tshane (dry) site with a mean value of 9.2 ‰, whereas the mean value at the Mongu (wet) site is 4.4 ‰ (Table 1). At Tshane the soil $\delta^{15}N$ is higher under trees or shrubs than in bare soil or beneath grasses; similar results were found at Mongu but with smaller differences (Table 1). Unlike the soil $\delta^{15}N$, the soil N content exhibits an opposite pattern:

it is lower at the Tshane (dry) site with a mean value of 0.02% and higher at the Mongu (wet) site with a mean of 0.04 ‰ (Table 1). These results are in agreement with previous findings from this region (Swap et al. 2004; Aranibar et al. 2008; Wang et al. 2009d; Wang et al. 2010a). The higher soil δ^{15}N values at Tshane generally indicate a more open N cycle (e.g., the ratio of N losses to internally cycled N is high) at the dry end, which likely result from higher N availability relative to N demand in more arid environments. δ^{15}N values at the dry site were found to be around 14 ‰ in a 2000 sampling (Aranibar et al. 2004), higher than that in the current study (9.2 ‰) and than another independent 2005 wet season sampling (10.4 ‰ for under canopy and 9.7 ‰ for open canopy areas, Wang et al. 2010a). These differences may be due to the different sampling location among these studies since the heterogeneity is large at the dry site. Water availability may, however, play a more important role. The year 2000 was wet and followed the 1999 drought. The sampling year (2005) of the current study is also a wet year with rainfall value of 436 mm (MAP of the site is 365 mm). Since both sampling years are wetter than the MAP, the higher δ^{15}N in 2000 is likely related to the dry-wet cycle in 1999 and 2000. It is possible that N gas loss is large in 2000 following heavy rainfall events because of the N buildup during the 1999 drought. The coefficient of variation (CV) of soil δ^{15}N is much lower at Tshane (24%) compared to Mongu (51%) (Table 1). The CVs of soil %N at the two sites are comparable with CV values of 65% and 61% at Tshane and Mongu, respectively (Table 1); these results are similar to those reported for soil %C in an earlier study (Wang et al. 2009c). The lower soil δ^{15}N CV value at the dry site is unexpected since resources are usually more heterogeneous at the dry end (Wang et al. 2007b). The lower spatial variability of soil δ^{15}N at the dry end is

probably due to the indistinct soil $\delta^{15}N$ values between under canopy and open canopy areas (Table 1), as found in an early report with a non-spatial explicit sampling design (Wang et al. 2007b). The large CV in soil $\delta^{15}N$ at the wet site (Mongu) is likely related to the rainfall situation of the sampling year (2005). The rainfall value (564 mm) is significantly lower than the MAP (about 900 mm). The drier condition at the wet site will make the water availability difference between open and under canopy areas larger, which will lead to higher $\delta^{15}N$ difference as water availability largely determines $\delta^{15}N$ in water-limited systems (Austin and Sala 1999; Aranibar et al. 2004; Wang et al. 2010a). The same principle but converse trend (higher rainfall and lower $\delta^{15}N$ CV value) applies to the dry site, as the rainfall amount is larger than the MAP at the drier site. There was larger difference in $NO_3^-+NO_2^-$ between under canopy and open canopy areas at the dry site compared with the wet site (Table 1), which is similar to the modeling study result in this region (Wang et al. 2009a). The soil moisture was higher at the wet site (~3%) than the dry site (~0.7%) but the differences between microhabitats were small at both sites (Table 1). The small difference at the dry site is unexpected, which is likely related to the fact that the low soil moisture (~0.7%) of the site is close to the sensor resolution (~1%).

Plant foliar $\delta^{15}N$ follows similar trends as the soil $\delta^{15}N$, with higher mean values (8.3 ‰ and 5.3 ‰ for C_3 and C_4 plants respectively) at the Tshane (dry) site and lower mean values (2.5 ‰ and 2.1 ‰ for C_3 and C_4 plants respectively) at the Mongu (wet) site (Table 2). Root $\delta^{15}N$ patterns are similar but the values are much lower than those of foliar and soil samples (Table 2). The pattern of lower plant $\delta^{15}N$ than soil $\delta^{15}N$ is similar to that found at the global scale (Amundson et al. 2003). The average foliar $\delta^{15}N$ value at Tshane is higher than those reported for Namib desert species with an average of 4.4‰

for N-fixing species (Schulze et al. 1991) and also higher than those found in a Tanzania savanna woodland (Hogberg 1986). The foliar δ^{15}N in N-fixing plants has been shown to be close to atmospheric δ^{15}N (0-2‰) (Shearer and Kohl 1986; Yoneyama et al. 1990). The average soil δ^{15}N under two potential N-fixing species in this study is 9.2‰ and 10.1‰ for *A. luederizii* and *A. mellifera*, respectively. The high soil δ^{15}N under the two *Acacia* species indicate that N-fixing may not be a major N source to this system, which is in agreement with earlier reports in southern Africa (Aranibar et al. 2004; Wang et al. 2010a; Wang et al. in press). Other studies have shown that some leguminous shrubs with nodules in their root systems do not appear to be active N fixers, though N fixation could occur in wetter years (Golluscio et al. 2006).

There appear to be well-defined spatial patterns for soil δ^{15}N at Tshane but not at Mongu. At Tshane the range of autocorrelation is similar for soil δ^{15}N and woody existence (Table 3; Figure 3), with estimated values of 15.4 m and 15.0 m, respectively (Figure 3a, 3c). At Mongu, the spatial structure of soil δ^{15}N is consistent with that of a nugget model (random pattern). Using spherical model we determine a range of autocorrelation in woody cover of 1.3 m at Mongu, although with a low R^2 of 0.06 (Figure 3b, d), indicating a random distribution. The $C/(C+C_o)$ values for soil δ^{15}N is lower than that of woody cover (Figure 3a, 3c) at the dry site, indicating that the degree of spatial dependence of soil δ^{15}N is less than that of woody cover.

At the dry site (Tshane), the spatial patterns of soil δ^{15}N are in agreement with those of woody plant presence, whereas the spatial distribution of soil δ^{15}N is different from that of snapshot soil moisture measurements, as suggested by the different ranges of autocorrelation of these two variables (Figure 3 and 4). The range of autocorrelation of

soil moisture is 344 m (Figure 4a), while the range of autocorrelation of soil δ^{15}N is 15.4 m, which indicates that snapshot soil moisture results do not explain the spatial structure of soil δ^{15}N at the dry site. At the wet site, soil moisture does not exhibit a spatial structure as suggested by the nugget model (Figure 4b, 4d). In addition, the correlation between soil moisture and soil δ^{15}N is not significant (Table 4), indicating that the snapshot soil moisture do not affect the spatial distribution of soil δ^{15}N at the wet site either. We should stress, however, that these soil moisture measurements were taken as snapshot of the soil water content at the time of soil sampling. Even though these data capture the higher soil moisture existing at the wet site (3.25% vs. 0.71% at the wet and dry end, respectively, Table 1), we cannot exclude that more significant within-site relations might be found between soil moisture and soil δ^{15}N if longer-term soil moisture measurements were available. Therefore, caution should be used before concluding that soil moisture does not contribute to the spatial patterns of soil δ^{15}N. Long-term records (e.g., a whole growing season) of soil moisture monitoring or the geochemical indicators reflecting a long-term soil water status such as carbonate-rich soil horizon layer depth may help assess whether a relationship with the spatial distribution of soil δ^{15}N exists. In fact, process-based modeling work has shown that soil moisture plays an important role in regulating the N cycles in drylands in general (D'Odorico et al. 2003) and in the Kalahari in particular (Wang et al. 2009a). Because ^{15}N is more sensitive than the total N changes, it is expected that soil moisture spatial distribution will affect the soil δ^{15}N spatial patterns.

There is a significant negative spatial correlation between grass cover and soil δ^{15}N both at the dry and at the wet site with correlation coefficients of -0.20 and -0.18 at

Tshane and Mongu, respectively (Table 4). This negative correlation is caused by the lower foliar $\delta^{15}N$ input from grasses under the grass canopy areas since grass foliar $\delta^{15}N$ is lower than woody species (Table 2). There is a significant negative spatial correlation between soil C/N ratios and soil $\delta^{15}N$ at the wet site with a correlation coefficient of -0.32 (Table 4), which is likely caused by the higher foliar and root C/N ratios and lower foliar and root $\delta^{15}N$ in grasses compared with woody species (Table 2). Such a negative correlation between soil C/N and soil $\delta^{15}N$ does not appear at the dry site. The pattern of root and foliar C/N and $\delta^{15}N$ between under canopy and open canopy areas is similar to that of the wet end, but other factors such as wind and water move soil and debris around and homogenize the landscape at the dry site, resulting in non-different soil $\delta^{15}N$ and C/N values between under canopy and open canopy areas (Table 1). This is probably the reason why a negative correlation between soil C/N and soil $\delta^{15}N$ is not found at the dry site. There is also a significant positive spatial correlation between soil %N and soil $\delta^{15}N$ at the dry site with a coefficient of 0.29 (Table 4), which is likely caused by the lower foliar and root %N and lower foliar/root $\delta^{15}N$ in grasses compared with woody species at the dry site (Table 2). Such a positive correlation between %N and soil $\delta^{15}N$ does not appear at the wet site because there is no difference in foliar $\delta^{15}N$ values between trees and grasses at the wet end (Wang et al. 2010a). There is no spatial correlation between $NO_3^-+NO_2^-$ and soil $\delta^{15}N$ both at the dry and wet site (Table 4), indicating these anions alone could not represent N transformation processes in these systems. Bare ground is negatively correlated with woody cover at both sites and with grass cover only at the dry site. There is no spatial correlation between bare ground and soil $\delta^{15}N$ but negative relationships exist for bare ground and soil %N at both sites (Table 4). Together with the

fact that %N spatial autocorrelation range is larger than that of soil δ^{15}N (Table 3), these results indicate that different mechanisms are responsible for the spatial patterns of soil δ^{15}N and soil %N.

To further explore the determinant factors of the spatial patterns of soil δ^{15}N, the spatial distribution of two potential N-fixing *Acacia* species (*A. luederizii* and *A. mellifera*) were compared with that of soil δ^{15}N. The range of autocorrelation of *A. luederizii* (Figure 3a, 5a) is closer to that of soil δ^{15}N (12.3 m vs. 15.4 m, respectively), whereas the autocorrelation range of *A. mellifera* is substantially different (2.7 m, Figure 3a, 5b). However, the distribution of both *Acacia* species have no significant correlation with that of soil δ^{15}N (Table 4), thereby strengthening the argument that N-fixation is not a major N source in this system, and therefore it does not affect the spatial pattern of soil δ^{15}N. It also indicates that *A. mellifera* plays a minor role in shaping up the soil δ^{15}N spatial patterns. The woody cover distribution is positively correlated with soil δ^{15}N, as well as with soil %N (Table 4). Together with the fact that no correlation exists for potential N-fixing trees, these results indicate that woody plants affect the spatial distribution of soil δ^{15}N not through N-fixation. The autocorrelation ranges of soil δ^{15}N and woody existence are similar, namely, 15.4 m and 15.0 m, respectively (Figure 4), while that of %N is 19.50 m (Table 3). The larger autocorrelation range for %N compared with woody existence indicates the plant root effect on %N since in water-limited systems root distribution is generally larger than the canopy size. It also indicates that factors influencing δ^{15}N are confined within tree canopy, but factors influencing %N are exceeding the canopy (e.g., root distribution). The factors influencing δ^{15}N include physical processes such as canopy shading, litter input, evaporation reduction, as well as

chemical processes such as the enhancement of mineralization, nitrification and denitrification. Litter inputs may also inhibit the development of soil crusts thereby causing a decrease in N fixation by cyanobacteria bare patches or under the grasses. The similar autocorrelation ranges of δ^{15}N and woody existence, however, indicate that these factors can be lumped together at ecosystem spatial scale. This result thus indicates that - in dry environments where the spatial distribution of woody vegetation determines the soil δ^{15}N spatial distribution - predicting ecosystem-scale patterns of soil δ^{15}N can be achieved through the quantification of woody vegetation spatial patterns.

4. Summary

Contrary to our first hypothesis, spatial patterns of soil δ^{15}N only exist at the dry site (Tshane), but not at the wet site (Mongu), which may result from less spatially structured woody plant distribution at the wet site. Consistent with our second hypothesis, based on the similar spatial distribution of woody vegetation and soil δ^{15}N, it is found that woody cover distribution affects soil δ^{15}N at the dry site; however, the two potential N-fixing species do not contribute the spatial pattern for soil δ^{15}N. This is explained by the very low N input from N-fixation under dry conditions suggested by the high foliar and soil δ^{15}N values. This result also indicates that woody vegetation affects the spatial distribution of soil δ^{15}N through N inputs and other transformation processes, not through N-fixation. Grass cover has negative correlations with the spatial pattern of soil δ^{15}N spatial pattern both at the dry and at the wet site because of the lower foliar δ^{15}N values of grasses compared with woody species. Contrary to our third hypothesis, soil moisture did not exhibit any control on the spatial pattern of soil δ^{15}N both at the dry and wet site,

presumably because soil moisture measurement were available only as "snapshots" and the time scale of soil moisture dynamics are different from those of δ^{15}N. Whereas previous studies showed a strong rainfall control on vegetation distribution and tree-grass interactions along the KT (Caylor et al. 2003; D'Odorico et al. 2007; Aranibar et al. 2008; Wang et al. 2010a), this study shows that both tree and grass distributions affect the spatial patterns of soil δ^{15}N at the dry end of the KT. The combined results suggest that water availability indirectly affects the spatial distribution of soil δ^{15}N through its effects on the distribution of woody vegetation and grass vegetation at the dry site.

Acknowledgements

The project was supported by NASA-IDS2 (NNG-04-GM71G). We greatly appreciate the field assistance and technical assistance from Natalie Mladenov, Lydia Ries, Beth Caylor, Junran Li, Dikitso Kolokose, O.G.S.O. Kgosidintsi, Thoralf Meyer and Kebonyethata Dintwe. Lixin Wang also acknowledges the financial support from Vice-Chancellor's postdoctoral research fellowship of University of New South Wales. We thank three anonymous reviewers of their constructive comments.

References

Amundson R, Austin AT, Schuur EAG et al (2003) Global patterns of the isotopic composition of soil and plant nitrogen. Global Biogeochemical Cycles 17(1):1031, doi:10.1029/2002GB001903

Aranibar JN, Anderson IC, Ringrose S, Macko SA (2003) Importance of nitrogen fixation in soil crusts of southern African arid ecosystems: acetylene reduction and stable isotope studies. Journal of Arid Environments 54:345-358

Aranibar JN, Otter L, Macko SA et al (2004) Nitrogen cycling in the soil-plant system along a precipitation gradient in the Kalahari sands. Global Change Biology 10(3):359-373

Aranibar JN, Anderson IC, Epstein HE et al (2008) Nitrogen isotope composition of soils, C_3 and C_4 plants along land use gradients in southern Africa. Journal of Arid Environments 72:326-337 doi:10.1016/j.jaridenv.2007.06.007
Austin AT, Sala OE (1999) Foliar d15N is negatively correlated with rainfall along the IGBP transect in Australia. Australian Journal of Plant Physiology 26:293-295
Austin AT, Yahdjian L, Stark JM et al (2004) Water pulses and biogeochemical cycles in arid and semiarid ecosystems. Oecologia 141(2):221-235
Bai E, Boutton TW, Liu F, Wu XB, Archer SR, Hallmark CT (2009) Spatial variation of the stable nitrogen isotope ratio of woody plants along a topoedaphic gradient in a subtropical savanna. Oecologia 159(3):493-503, DOI: 10.1007/s00442-008-1246-0
Brooker PI (1991) A geostatistical primer. World Scientific Publishing Co. Pte. Ltd, Singapore
Caylor KK, Shugart HH, Dowty PR, Smith TM (2003) Tree spacing along the Kalahari transect in southern Africa. Journal of Arid Environments 54:281-296
Cheng W, Chen Q, Xu Y, Han X, Li L (2009) Climate and ecosystem ^{15}N natural abundance along a transect of Inner Mongolian grasslands: Contrasting regional patterns and global patterns. Global Biogeochemical Cycles 23:GB2005, doi:10.1029/2008GB003315
D'Odorico P, Laio F, Porporato A, Rodriguez-Iturbe I (2003) Hydrologic control on soil carbon and nitrogen cycles, II A case study. Advances in Water Resources 26:59-70
D'Odorico P, Caylor K, Okin GS, Scanlon TM (2007) On soil moisture-vegetation feedbacks and their possible effects on the dynamics of dryland ecosystems. Journal of Geophysical Research 112:G04010, doi:10.1029/2006JG000379
Davis JC (2002) Statistics and data analysis in geology. John Wiley & Sons, New York
Elmore AJ, Craine JM (2011) Spectroscopic analysis of canopy nitrogen and nitrogen isotopes in Managed pastures and hay land. Geoscience and Remote Sensing, IEEE Transactions on 49(7):2491-2498
Evans R, Ehleringer J (1993) A break in the nitrogen cycle in aridlands? Evidence from ^{15}N of soils. Oecologia 94:314-317
Garten C, Van Miegroet H (1994) Relationships between soil nitrogen dynamics and natural ^{15}N abundance in plant foliage from Great Smoky Mountains National Park. Can J For Res 24:1636-1645
Garten CT (1993) Variation in foliar ^{15}N abundance and the availability of soil nitrogen on walker branch watershed Ecology 74(7):2098-2113
Golluscio R, Faigón A, Tanke M (2006) Spatial distribution of roots and nodules, and $\delta^{15}N$ evidence of nitrogen fixation in *Adesmia volckmanni*, a Patagonian leguminous shrub. Journal of Arid Environments 67:328-335
Hogberg P (1986) Nitrogen fixation and nutrient relations in savanna woodland trees (Tanzania). Journal of Applied Ecology 23:675-688
Högberg P (1997) ^{15}N natural abundance in soil-plant systems New Phytologist 137(2):179-203
Koch GW, Scholes RJ, Steffen WL, Vitousek PM, Walker BH (1995) The IGBP terrestrial transects: Science plan, Report No. 36. International Geosphere-Biosphere Programme, Stockholm

Li J, Okin G, Alvarez L, Epstein H (2008) Effects of wind erosion on the spatial heterogeneity of soil nutrients in two desert grassland communities. Biogeochemistry 88:73-88
Li J, Richter Dd, Mendoza A, Heine P (2010) Effects of land-use history on soil spatial heterogeneity of macro- and trace elements in the Southern Piedmont USA. Geoderma 156(1-2):60-73
Okin GS, Mladenov N, Wang L et al (2008) Spatial patterns of soil nutrients in two southern African savannas. Journal of Geophysical Research-Biogeosciences 113:G02011, doi:10.1029/2007JG000584
Pardo L, McNulty S, Boggs J, Duke S (2007) Regional patterns in foliar 15N across a gradient of nitrogen deposition in the northeastern US. Environmental Pollution 149:293-302
Pardo-Iguzquiza E, Dowd P (2001) Variance-covariance matrix of the experimental variogram: Assessing variogram uncertainty. Mathematical Geology 33(4):397-419
Robinson D (2001) $\delta^{15}N$ as an integrator of the nitrogen cycle. Trends in Ecology and Evolution 16:153-162
Rosenberg MS, Anderson CD (2011) PASSaGE: Pattern Analysis, Spatial Statistics and Geographic Exegesis. Version 2. Methods in Ecology and Evolution 2(3):229-232
Schlesinger WH, Raikes JA, Hartley AE, Cross AF (1996) On the spatial pattern of soil nutrients in desert ecosystems. Ecology 77(2):364-374
Schulze E-D, Gebauer G, Ziegler H, Lange OL (1991) Estimates of nitrogen fixation by trees on an aridity gradient in Namibia. Oecologia 88:451-455
Shearer G, Kohl D (1986) N_2-fixation in field settings: estimations based on natural ^{15}N abundance. Austral J Plant Physiol 13:699-756
Su Y, Li Y, Zhao H (2006) Soil properties and their spatial pattern in a degraded sandy grassland under post-grazing restoration, Inner Mongolia, northern China. Biogeochemistry 79(3):297-314
Swap RJ, Aranibar JN, Dowty PR, Gilhooly WP, Macko SA (2004) Natural abundance of ^{13}C and ^{15}N in C_3 and C_4 vegetation of southern Africa: patterns and implications. Global Change Biology 10(3):350-358
Thomas AD, Hoon SR, Linton PE (2008) Carbon dioxide fluxes from cyanobacteria crusted soils in the Kalahari. Applied Soil Ecology 39:254-263
Wang L, Okin GS, Wang J, Epstein H, Macko SA (2007a) Predicting leaf and canopy ^{15}N compositions from reflectance spectra. Geophysical Research Letters 34:L02401
Wang L, D'Odorico P, Ringrose S, Coetzee S, Macko S (2007b) Biogeochemistry of Kalahari sands. Journal of Arid Environments 71(3):259-279 doi:10.1016/j.jaridenv.2007.03.016
Wang L, Mou PP, Huang J, Wang J (2007c) Spatial heterogeneity of soil nitrogen in a subtropical forest in China. Plant and Soil 295:137-150
Wang L, D'Odorico P, Manzoni S, Porporato A, Macko S (2009a) Carbon and nitrogen dynamics in southern African savannas: the effect of vegetation-induced patch-scale heterogeneities and large scale rainfall gradients. Climatic Change 94:63-76
Wang L, Okin G, Macko S (2009b) Remote sensing of nitrogen and carbon isotope compositions in terrestrial ecosystems. In: West J, Bowen G, Tu K, Dawson T. (Eds.),

Isoscapes: Understanding movement, pattern and process on Earth through isotope mapping. Springer, pp. 51-70.
Wang L, Okin GS, Caylor KK, Macko SA (2009c) Spatial heterogeneity and sources of soil carbon in southern African savannas. Geoderma 149:402-408, doi:10.1016/j.geoderma.2008.12.014
Wang L, D'Odorico P, Okin G, Macko S (2009d) Isotope composition and anion chemistry of soil profiles along the Kalahari Transect. Journal of Arid Environments 73:480-486, doi:10.1016/j.jaridenv.2008.11.010
Wang L, D'Odorico P, Ries L, Macko S (2010a) Patterns and implications of plant-soil $\delta^{13}C$ and $\delta^{15}N$ values in African savanna ecosystems. Quaternary Research 73:77-83, DOI: 10.1016/j.yqres.2008.11.004
Wang L, D'Odorico P, Ries L, Caylor K, Macko S (2010b) Combined effects of soil moisture and nitrogen availability variations on grass productivity in African savannas. Plant and Soil 328:95-108, 10.1007/s11104-009-0085-z
Wang L, Katjiua M, D'Odorico P, Okin GS (in press) The interactive nutrient and water effects on vegetation biomass at two African savanna sites with different mean annual precipitation. African Journal of Ecology:doi: 10.1111/j.1365-2028.2012.01339.x
Yoneyama T, Murakami T, Boonkerd N, Wadisirisuk P, Siripin S, Kouno K (1990) Natural ^{15}N abundance in shrub and tree legumes, Casuarina, and non N_2 fixing plants in Thailand. Plant and Soil 128:287-292

Table 1. Mean value and coefficient of variation (CV) of soil $\delta^{15}N$, %N, C/N, $NO_3^-+NO_2^-$ (mg/g) and volumetric soil moisture (%) at Tshane (dry) and Mongu (wet). The %N, C/N and $NO_3^-+NO_2^-$ data have been reported in Okin et al. (2008) and were used here to facilitate the interpretations of soil $\delta^{15}N$ spatial pattern.

Location		$\delta^{15}N$ (‰)		%N		C/N		$NO_3^-+NO_2^-$ (mg/g)		Soil moisture (%)	
		Mean	CV	Mean	CV	Mean	CV	Mean	CV	Mean	CV
Tshane (Dry)	All samples	9.2	0.24	0.023	0.65	8.34	0.10	1.79	2.36	0.71	0.78
	Tree/Shrub	9.9a	0.20	0.044a	0.42	8.18a	0.12	4.55a	1.37	0.58a	0.89
	Grass	8.9b	0.26	0.021b	0.37	8.35a	0.08	1.39b	2.27	0.65a	0.91
	Bare	9.3ab	0.20	0.019b	0.45	8.05a	0.08	1.24b	2.09	0.91a	0.58
Mongu (Wet)	All samples	4.4	0.51	0.039	0.61	17.82	0.10	3.44	1.03	3.25	0.20
	Tree/Shrub	4.3a	0.49	0.041a	0.58	17.97a	0.11	3.13a	1.16	3.12a	0.15
	Grass	2.6b	0.74	0.032a	-	18.66a	-	10.1	-	3.00a	0.24
	Bare	4.8a	0.61	0.028b	0.66	17.88a	0.09	4.51a	0.68	3.17a	0.12

Note: The same letters indicate the same mean for different microhabitats (e.g., tree/shrub, grass and bare) within the same site at α=0.05.

Table 2. Summary of statistical parameters of plant $\delta^{15}N$, %N and C/N at Tshane (dry) and Mongu (wet).

Location		$\delta^{15}N$ (‰)		%N		C/N	
		Mean	CV	Mean	CV	Mean	CV
Tshane (Dry)	C_3 leaves	8.3	0.16	3.17	0.079	14.12	0.072
	C_3 roots (0-30cm)	5.5	0.25	1.74	0.20	19.39	0.092
	C_3 roots (30-50 cm)	2.0	0.26	1.70	0.12	26.31	0.14
	C_4 leaves	5.3	0.26	2.27	0.26	20.74	0.22
	C_4 roots (0-30 cm)	1.1	1.1	0.82	0.33	59.80	0.27
Mongu (Wet)	C_3 leaves	2.5	0.25	2.37	0.070	21.94	0.051
	C_3 roots (0-30cm)	2.0	0.97	1.60	0.20	28.75	0.35
	C_3 roots (30-50 cm)	-1.3	-0.52	1.08	0.13	45.14	0.15
	C_4 leaves	2.1	1.1	0.84	1.06	28.35	0.042
	C_4 roots (0-30 cm)	0.9	0.8	0.68	0.40	59.95	0.036

Table 3. Range (m) and proportion of structured variance ($C/(C_o+ C)$) for variograms from both sites. "M" denote the mean jackknife estimate. "L" and "U" denote the lower and upper bounds of the 95% confidence estimates, respectively. The %N, and NO_3^- $+NO_2^-$ data have been reported in Okin et al. (2008) and were re-analyzed here using exponential model for Tshane to facilitate the comparison with soil $\delta^{15}N$ spatial pattern.

Location	Analyte	Range (m)			$C/(C_o+C)$		
		M	L	U	M	L	U
Tshane (Dry)	$\delta^{15}N$	15.40	15.08	15.72	0.38	0.34	0.41
	%N	19.50	19.16	19.84	0.34	0.32	0.37
	$NO_3^-+NO_2^-$	4.31	4.14	4.48	0.01	-0.05	0.08
Mongu (Wet)	$\delta^{15}N$	Nugget model					
	%N	4.77	4.59	4.95	0.64	0.59	0.68
	$NO_3^-+NO_2^-$	Nugget model					

Table 4. Correlations of soil $\delta^{15}N$, %N, C/N, $NO_3^-+NO_2^-$, volumetric soil moisture, woody distribution, grass distribution and *Acacia* tree distribution (Tshane only) at Tshane (dry) and Mongu (wet). The correlations were calculated using a modified *t*-test that corrects the degrees of freedom based on the amount of auto-correlation in the data (e.g., Wang et al. 2007). The %N, C/N and $NO_3^-+NO_2^-$ data have been reported in Okin et al. (2008) and were used here to facilitate the interpretations of soil $\delta^{15}N$ spatial pattern.

		$\delta^{15}N$ (‰)	%N	C/N	$NO_3^-+NO_2^-$	Moisture	Woody	Grass	ALE	AME	ALE/AME	Bare
Tshane (Dry)	$\delta^{15}N$ (‰)	1	-	-	-	-	-	-	-	-	-	
	%N	0.29**	1	-	-	-	-	-	-	-	-	
	C/N	-0.04	0.11	1	-	-	-	-	-	-	-	
	$NO_3^-+NO_2^-$	-0.04	-0.08	0.08	1	-	-	-	-	-	-	
	Moisture	-0.0008	-0.02	-0.07	0.10	1	-	-	-	-	-	
	Woody	0.25**	0.52***	0.19*	-0.07*	-0.16	1	-	-	-	-	
	Grass	-0.20**	-0.42**	0.07	-0.09	-0.11	-0.31***	1	-	-	-	
	ALE	-0.01	0.47***	0.35***	0.04	0.13	0.42***	-0.20*	1	-	-	
	AME	0.10	0.06	-0.03	-0.03	-0.04	0.29***	-0.11	-0.08	1	-	
	ALE/AME	0.05	0.43***	0.28***	0.02	0.02	0.53***	-0.24**	0.79***	0.54***	1	
	Bare	-0.003	-0.13*	-0.14*	-0.0099	0.13	-0.28***	-0.53***	-0.12	-0.08	-0.15*	1
Mongu (Wet)	$\delta^{15}N$ (‰)	1	-	-	-	-	-	-	-	-	-	
	%N	-0.08	1	-	-	-	-	-	-	-	-	
	C/N	-0.32***	0.22**	1	-	-	-	-	-	-	-	
	$NO_3^-+NO_2^-$	-0.02	0.08	-0.05	1	-	-	-	-	-	-	
	Moisture	0.02	-0.02	-0.007	0.20	1	-	-	-	-	-	
	Woody	-0.07	0.14	0.04	0.002	-0.03	1		-	-	-	
	Grass	-0.18*	-0.12	-0.019	-0.06	-0.10	0.08	1	-	-	-	
	Bare	0.12	-0.15*	-0.056	0.0026	0.030	-1.0***	-0.078	-	-	-	1

ALE: *Acacia luederizii*, AME: *Acacia mellifera*

*P < 0.05 , **P < 0.01, ***P < 0.001

Figure 1. Sampling locations and vegetation characteristics along the Kalahari Transect. The satellite images of each site are IKONOS (Tshane) and Quickbird (Mongu).

Figure 2. Ecosystem-scale variations of $\delta^{15}N$ (A), soil %N (B), soil C/N (C), soil NO_3^- $+NO_2^-$ (D) and soil moisture (E) at Tshane and Mongu. The %N, C/N and $NO_3^-+NO_2^-$ data have been reported in Okin et al. (2008) and were used here to facilitate the interpretations of soil $\delta^{15}N$ spatial pattern.

Figure 3. Semivariograms of $\delta^{15}N$ at Tshane (A), Mongu (B), and semivariograms of woody cover at Tshane (C) and Mongu (D) along the Kalahari Transect. The summary of semivariogram model parameters is reported under the curve. Proportion structural variation ($C/(C + C_o)$) is used as an index of the magnitude of spatial dependence.

Figure 4. Semivariograms of soil moisture at Tshane (A), Mongu (B), and semivariograms of grass cover at Tshane (C) and Mongu (D) along the Kalahari Transect. The summary of semivariogram model parameters is reported under the curve.

Figure 5. Semivariograms of *Acacia leuderitzii* alone (A), *Acacia mellifera* alone (B) and the combination of the two (C) at Tshane. The summary of semivariogram model parameters is reported under the curve.

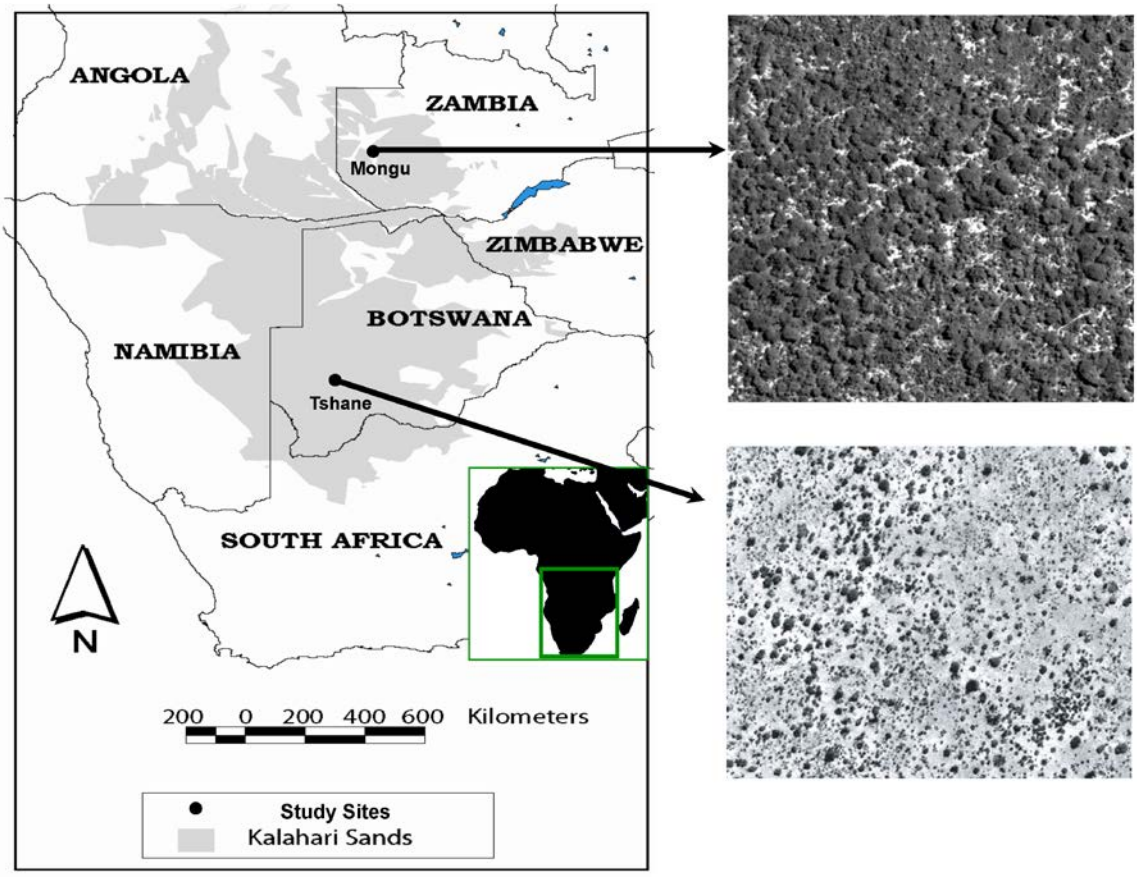
ANGOLA
ZAMBIA
Mongu
ZIMBABWE
BOTSWANA
NAMIBIA
Tshane
SOUTH AFRICA
N
200 0 200 400 600 Kilometers
Study Sites
Kalahari Sands

Figure 1.

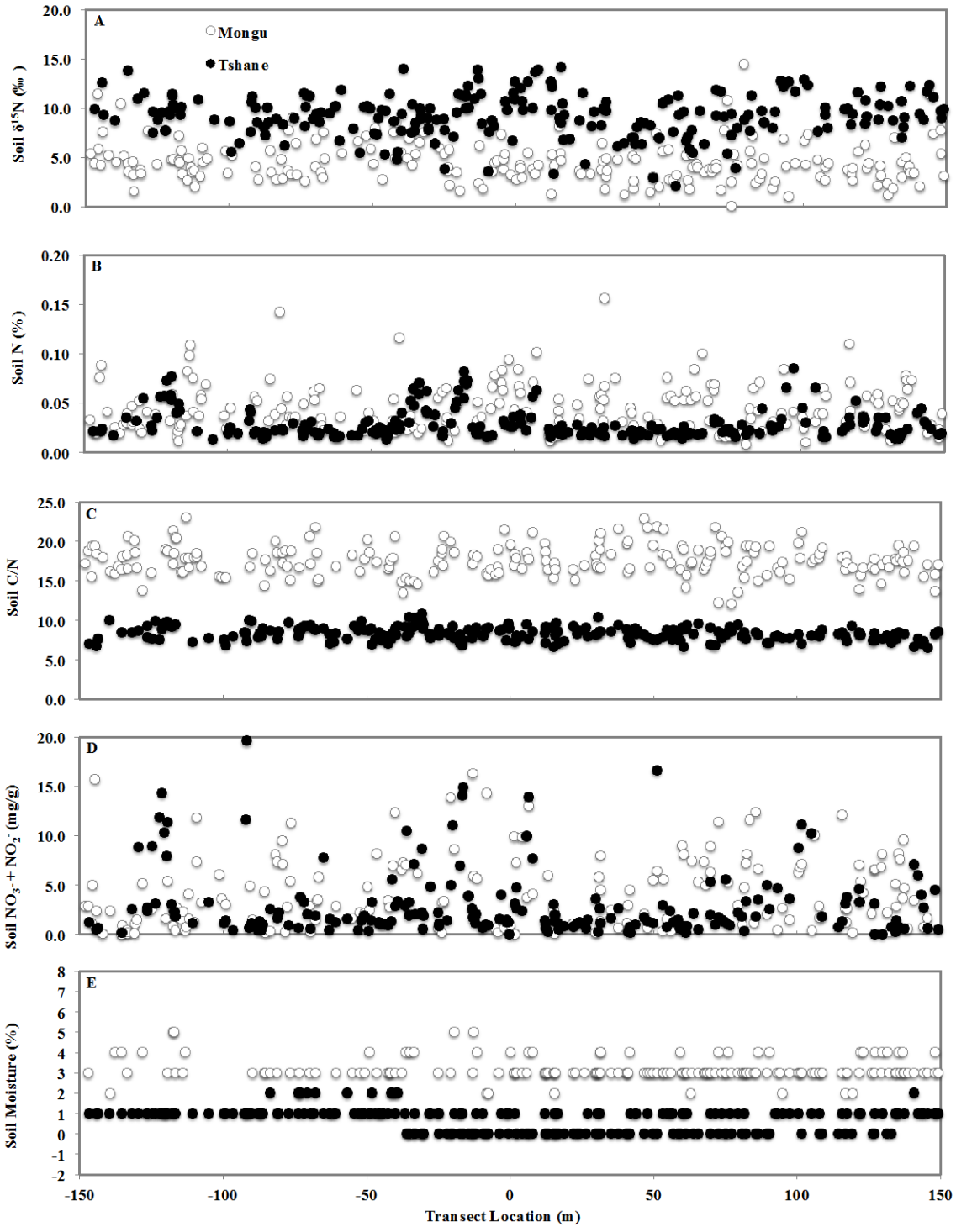
A
Mongu
Tshane
Soil δ15N (‰)
20.0
15.0
10.0
5.0
0.0
B
Soil N (%)
0.20
0.15
0.10
0.05
0.00
C
Soil C/N
25.0
20.0
15.0
10.0
5.0
0.0
D
Soil NO3- + NO2- (mg/g)
20.0
15.0
10.0
5.0
0.0
E
Soil Moisture (%)
8
7
6
5
4
3
2
1
0
-1
-2
-150
-100
-50
0
50
100
150
Transect Location (m)

Figure 2

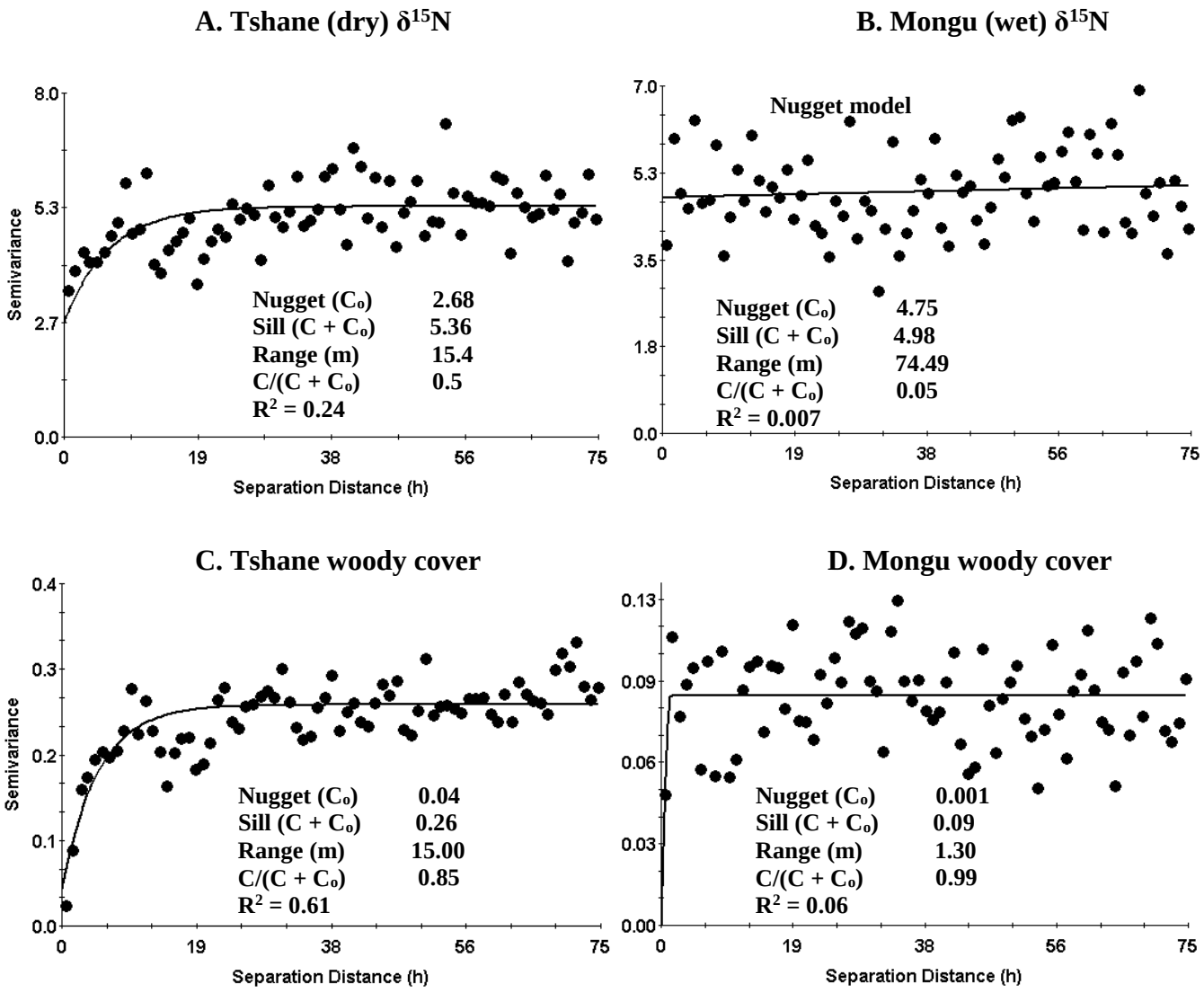
A. Tshane (dry) δ15N
B. Mongu (wet) δ15N
Nugget model
Semivariance
Separation Distance (h)
Nugget (C0) 2.68
Sill (C + C0) 5.36
Range (m) 15.4
C/(C + C0) 0.5
R2 = 0.24
Nugget (C0) 4.75
Sill (C + C0) 4.98
Range (m) 74.49
C/(C + C0) 0.05
R2 = 0.007
C. Tshane woody cover
D. Mongu woody cover
Nugget (C0) 0.04
Sill (C + C0) 0.26
Range (m) 15.00
C/(C + C0) 0.85
R2 = 0.61
Nugget (C0) 0.001
Sill (C + C0) 0.09
Range (m) 1.30
C/(C + C0) 0.99
R2 = 0.06

Figure 3.

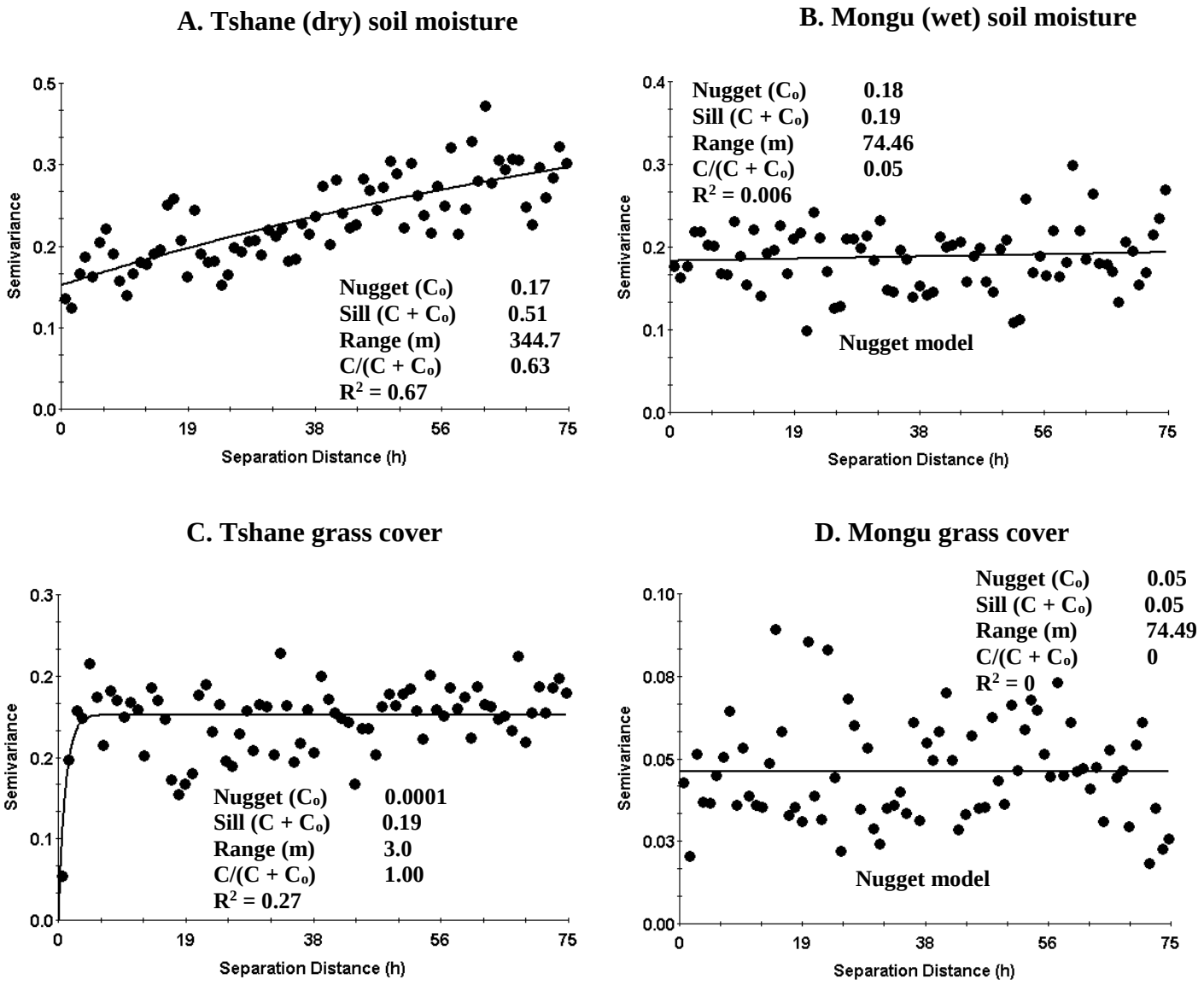
A. Tshane (dry) soil moisture
B. Mongu (wet) soil moisture
C. Tshane grass cover
D. Mongu grass cover
Semivariance
Separation Distance (h)
Nugget (C₀) 0.17
Sill (C + C₀) 0.51
Range (m) 344.7
C/(C + C₀) 0.63
R² = 0.67
Nugget (C₀) 0.18
Sill (C + C₀) 0.19
Range (m) 74.46
C/(C + C₀) 0.05
R² = 0.006
Nugget model
Nugget (C₀) 0.0001
Sill (C + C₀) 0.19
Range (m) 3.0
C/(C + C₀) 1.00
R² = 0.27
Nugget (C₀) 0.05
Sill (C + C₀) 0.05
Range (m) 74.49
C/(C + C₀) 0
R² = 0
Nugget model

Figure 4.

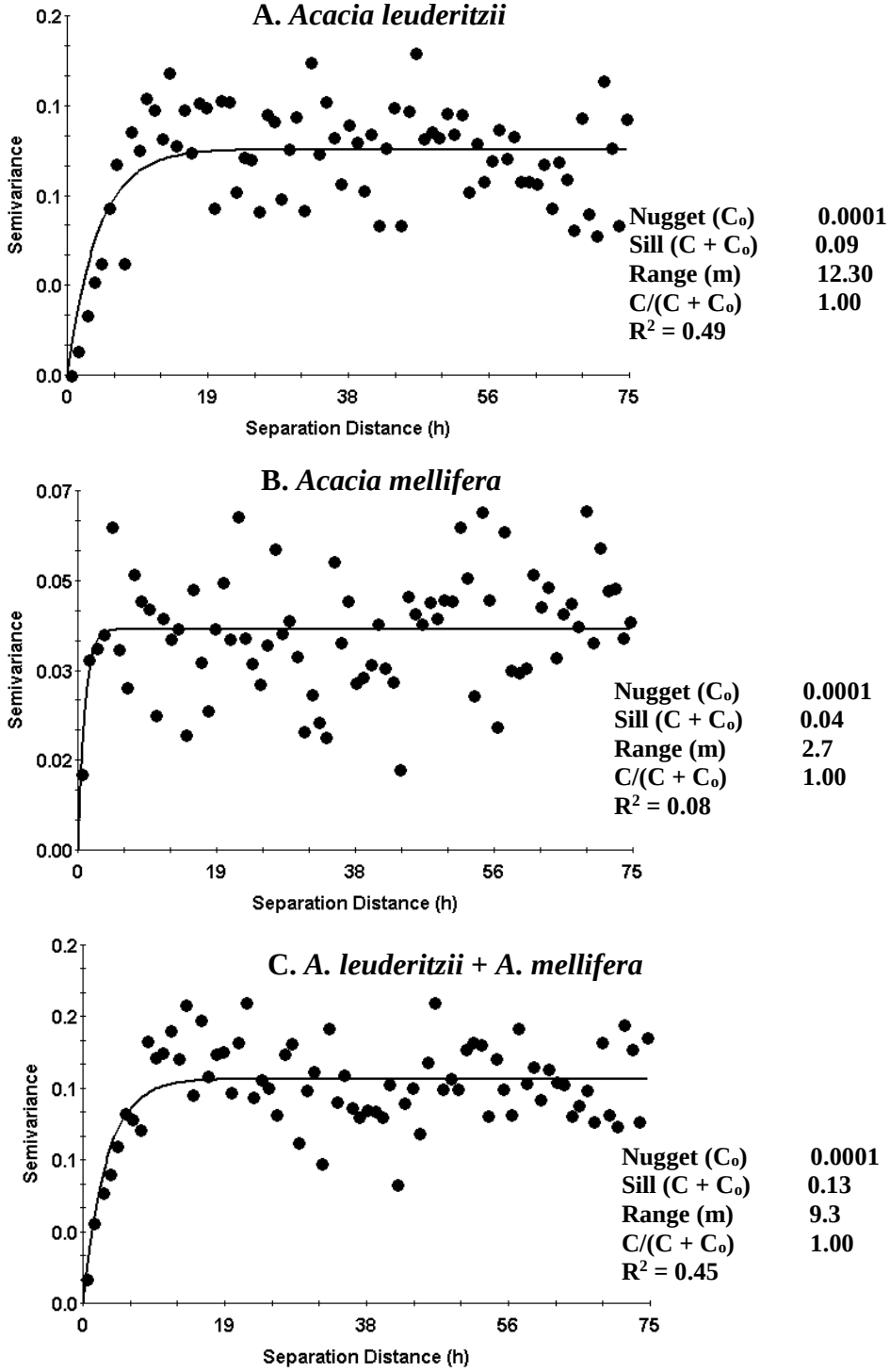
A. Acacia leuderitzii
Semivariance
Separation Distance (h)
Nugget (C₀) 0.0001
Sill (C + C₀) 0.09
Range (m) 12.30
C/(C + C₀) 1.00
R² = 0.49
B. Acacia mellifera
Semivariance
Separation Distance (h)
Nugget (C₀) 0.0001
Sill (C + C₀) 0.04
Range (m) 2.7
C/(C + C₀) 1.00
R² = 0.08
C. A. leuderitzii + A. mellifera
Semivariance
Separation Distance (h)
Nugget (C₀) 0.0001
Sill (C + C₀) 0.13
Range (m) 9.3
C/(C + C₀) 1.00
R² = 0.45

Figure 5.